NeuroImage: Clinical 35 (2022) 103095

Contents lists available at ScienceDirect

NeuroImage: Clinical

journal homepage: www.elsevier.com/locate/ynicl

The progressive loss of brain network fingerprints in Amyotrophic Lateral Sclerosis predicts clinical impairment

Antonella Romano [a,1], Emahnuel Trosi Lopez [a,1], Marianna Liparoti [b], Arianna Polverino [c], Roberta Minino [a], Francesca Trojsi [d], Simona Bonavita [d], Laura Mandolesi [e], Carmine Granata [f], Enrico Amico [g,h], Giuseppe Sorrentino [a,c,f,*], Pierpaolo Sorrentino [f,i]

[a] Department of Motor Sciences and Wellness - University of Naples "Parthenope", via Medina 40, 80133 Naples, Italy
[b] Department of Social and Developmental Psychology, University of Rome "Sapienza", Italy
[c] Institute of Diagnosis and Treatment Hermitage Capodimonte, via Cupa delle Tozzole 2, 80131 Naples, Italy
[d] Department of Advanced Medical and Surgical Sciences, Division of Neurology, University of Campania "Luigi Vanvitelli", Naples, Italy
[e] Department of Humanistic Studies, University of Naples Federico II, via Porta di Massa 1, 80133, Naples, Italy
[f] Institute of Applied Sciences and Intelligent Systems, CNR, via Campi Flegrei 34, 80078 Pozzuoli, NA, Italy
[g] Institute of Bioengineering, Center for Neuroprosthetics, EPFL, Geneva, Switzerland
[h] Department of Radiology and Medical Informatics, University of Geneva (UNIGE), Geneva, Switzerland
[i] Institut de Neurosciences des Systèmes, Aix-Marseille Université, Marseille, France

ARTICLE INFO

Keywords:
Clinical connectome fingerprint
Functional connectome
Brain network identifiability
Neurodegenerative diseases
Motor neurons disease
Magnetoencephalography, Phase Linearity Measurement

ABSTRACT

Amyotrophic lateral sclerosis (ALS) is a neurodegenerative disease characterised by functional connectivity alterations in both motor and extra-motor brain regions. Within the framework of network analysis, fingerprinting represents a reliable approach to assess subject-specific connectivity features within a given population (healthy or diseased). Here, we applied the Clinical Connectome Fingerprint (CCF) analysis to source-reconstructed magnetoencephalography (MEG) signals in a cohort of seventy-eight subjects: thirty-nine ALS patients and thirty-nine healthy controls. We set out to develop an identifiability matrix to assess the extent to which each patient was recognisable based on his/her connectome, as compared to healthy controls. The analysis was performed in the five canonical frequency bands. Then, we built a multilinear regression model to test the ability of the "clinical fingerprint" to predict the clinical evolution of the disease, as assessed by the Amyotrophic Lateral Sclerosis Functional Rating Scale-Revised (ALSFRS-r), the King's disease staging system, and the Milano-Torino Staging (MiToS) disease staging system. We found a drop in the identifiability of patients in the alpha band compared to the healthy controls. Furthermore, the "clinical fingerprint" was predictive of the ALSFRS-r ($p = 0.0397$; $\beta = 32.8$), the King's ($p = 0.0001$; $\beta = -7.40$), and the MiToS ($p = 0.0025$; $\beta = -4.9$) scores. Accordingly, it negatively correlated with the King's (Spearman's rho = -0.6041, $p = 0.0003$) and MiToS scales (Spearman's rho = −0.4953, $p = 0.0040$). Our results demonstrated the ability of the CCF approach to predict the individual motor impairment in patients affected by ALS. Given the subject-specificity of our approach, we hope to further exploit it to improve disease management.

1. Introduction

Since Charcot's first comprehensive anatomo-clinical description in 1874 (Rowland, 2001), Amyotrophic Lateral Sclerosis (ALS) has been defined as a neurodegenerative disease affecting both upper and lower motor neurons. More recently, clinical, molecular, and neuroimaging evidence suggest that ALS spreads well beyond the motor system (Agosta et al., 2016; Bersano et al., 2020). Besides motor impairment,

Abbreviations: ALS, Amyotrophic Lateral Sclerosis; MEG, Magnetoencephalography; FC, Functional Connectome; CCF, Clinical Connectome Fingerprint; PLM, Phase linearity measurement; ALSFRS-r, Amyotrophic Lateral Sclerosis Functional Rating Scale-Revised; MiToS, Milano-Torino Staging disease staging system; ROIs, Region of interest; IM, Identifiability matrix; ICC, Intra-class correlation coefficient; SR, Success rate; LOOCV, Leave-one-out-cross validation.

* Corresponding author at: Department of Motor Sciences and Wellness - University of Naples "Parthenope", Naples, Italy.
E-mail address: giuseppe.sorrentino@uniparthenope.it (G. Sorrentino).

[1] Antonella Romano and Emahnuel Troisi Lopez equally contributed to this work and shared first authorship.

https://doi.org/10.1016/j.nicl.2022.103095
Received 17 January 2022; Received in revised form 31 May 2022; Accepted 19 June 2022
Available online 23 June 2022

almost 50% of ALS patients show extra-motor symptoms which involve the cognitive (Goldstein and Abrahams, 2013) and behavioural (Phukan et al., 2007) domains, resulting in a clinical picture that overlaps with frontotemporal dementia (FTD) (Lomen-Hoerth et al., 2002), which is also confirmed by the presence of TDP-43 protein inclusions in several brain regions in both ALS and FTD patients (Geser et al., 2008; Rademakers et al., 2012).

In this regard, neuroimaging techniques such as f-MRI, PET, and SPECT, have been used to investigate functional connectivity modifications in ALS patients (Sorrentino et al., 2018; Trojsi et al., 2012; Turner et al., 2012). Mohammedi et al., found that the resting-state functional connectivity alterations mainly occur in the default mode and the sensori-motor networks (Mohammadi et al., 2009). These changes were correlated with the decline of the motor functions (Fraschini et al., 2018). Similarly, Verstrate et al., through f-MRI analysis, highlighted increased functional connectivity in the motor network which was reflected in a more rapid disease progression (Verstraete et al., 2011). In addition, a magnetoencephalography (MEG) study showed a widespread topological reorganisation of the brain network in the ALS, which becomes more connected as the disease progresses (Sorrentino et al., 2018). Taken together, these observations highlight the possible role of brain functional connectivity analysis in monitoring disease progression (Iturria-Medina and Evans, 2015), and, consequently, in refining diagnosis, improving clinical management, and setting up biomarkers to test disease-modifying drugs. However, the predictive capacity of these approaches over the individual clinical condition was generally not tested or provided only minor contribution.

Fingerprinting analysis based on the functional connectomes (FC) is a methodological approach utilised to define the subject-specific characteristics of each individual (Amico and Goñi, 2018; Finn et al., 2015; Sareen et al., 2021). It has been tested in both clinical and healthy populations, revealing that individuals affected by neurodegenerative diseases showed reduced identifiability with respect to healthy individuals (Sorrentino et al., 2021b; Svaldi et al., 2021). Interestingly, the reduced identifiability could predict individual clinical features of patients, leading to the concept of the Clinical Connectome Fingerprint (CCF) (Sorrentino et al., 2021b). In particular, investigating the MEG-based FCs of subjects affected by mild cognitive impairment (MCI) and of healthy controls, Sorrentino et al. (Sorrentino et al., 2021b) built an identification score based on the similarity between FCs of patients and healthy subjects (I-clinical), which predicted the patients' individual cognitive decline.

In the present study, we hypothesised that the global rearrangement of the brain connectivity occurring in ALS (Menke et al., 2017; Sorrentino et al., 2018; Zhou et al., 2016) led to a reduction in brain identifiability that, in turn, may be related to the clinical severity of disease. Hence, we hypothesise that the CCF could be exploited to extract connectome features which are useful to predict the individual clinical impairments in ALS patients. In order to test our hypothesis, we applied the CCF to source-reconstructed magnetoencephalography (MEG) data in a cohort of seventy-eight subjects, including thirty-nine ALS patients and thirty-nine healthy controls. The functional connectomes were obtained through the phase linearity measurement (PLM), a metric that quantifies the synchrony between pairs of MEG signals (Baselice et al., 2018). Subsequently, based on the frequency-specific PLM-based connectomes, we assessed the identifiability rate for both patients and controls, under the hypothesis that stereotyped brain dynamics would result into less recognisable FCs in patients as compared to controls. Finally, to determine whether the level of identifiability in patients was linked to the clinical condition, we calculated the I-clinical score, which provides individual information about the similarity of each patient's FC to the average FC of the control group. We tested the predictive power of the I-clinical with respect to the three main clinical ALS scales. In particular, we considered the Total Amyotrophic Lateral Sclerosis Functional Rating Scale-Revised (ALSFRS-r), which is used to assess the patients' clinical status; (Cedarbaum et al., 1999), the King's (Balendra et al., 2019) and Milano-Torino Staging (MiToS) (Fang et al., 2017) disease staging systems, which both take into account the chronological onset of symptoms.

2. Methods

2.1. Participants

Thirty-nine ALS patients (29 males and 10 females; mean age 59.63; SD ± 12.87; mean education 10.38 years SD ± 4.3) were recruited for this study. ALS was diagnosed according to the revised El-Escorial criteria (Brooks, 1994). None of the patients showed mutations in any of the following genes: SOD1, TARDBP, FUS/TLS, and C9ORF72. Inclusion criteria were: 1) no major medical illness and no use of substances that could interfere with MEG signals; (2) no other major systemic, psychiatric, or neurological diseases; and (3) no focal or diffuse brain damage reported at MRI assessment. The control group was composed of thirty-nine subjects (28 males and 11 females) matched for age (64 ± 10.4) and education (12 ± 4.3). The patients' group also underwent a neurophysiological and motor screening (see Table 1). The total Amyotrophic Lateral Sclerosis Functional Rating Scale-Revised (ALSFRS-r) was used to assess the patient's physical functions (the greater the score, the better the clinical conditions); the King's disease staging system and the Milano-Torino staging system (MiToS) were used to measure disease staging. The study protocol was approved by the Local Ethics Committee (University of Campania "Luigi Vanvitelli") with the protocol number 591/2018, and all participants provided written informed consent in accordance with the Declaration of Helsinki.

2.2. MRI acquisition

MR images of both healthy subjects and patients were acquired on a 3 T scanner equipped with an eight-channel parallel head coil (GE Healthcare, Milwaukee, WI, USA). Specifically, three-dimensional T1-weighted images (Gradient-echo sequence Inversion Recovery prepared Fast Spoiled Gradient Recalled-echo, time repetition = 6988 ms, TI = 1100 ms, TE = 3.9 ms, flip angle = 10, voxel size = 1 × 1 × 1.2 mm^3) were acquired. A standard template was used for those participants (six patients and nine healthy controls) who did not complete the MRI.

2.3. MEG acquisition

Data were acquired using a MEG system composed of 154 magnetometers SQUID (superconductive quantum interference device) and 9 reference sensors. The acquisition took place in a magnetically shielded room (ATB, Biomag, ULM, Germany) to reduce external noise. To define the position of the head under the helmet we used Fastrack (Polhemus®), that digitised the positions of four anatomical landmarks (nasion, right and left pre-auricular points and vertex of the head) and the position of four reference coils (attached to the head of the subject). Each subject was recorded twice (3.5 min each) with a one-minute break, in resting state with closed eyes. Electrocardiography (ECG)

Table 1
Cohort features (mean and standard deviation).

Parameters	ALS group	HC group
	N = 39	N = 39
Age (years)	59.53 (±12.87)	64.00 (±10.47)
Male/Female	29/10	28/11
Education (years)	10.38 (±4.3)	12.00 (±4.45)
Disease duration (months)	51.82 (±59.61)	
ALSFRS-r score (mean ± SD)	37 (±7.82)	
King's score (mean ± SD)	2.4 (±1.01)	
MiToS score (mean ± SD)	2.25 (±0.88)	

ALS = Amyotrophic lateral sclerosis; HC = healthy controls; ALSFRS-r = ALS functional rating scale-revised; MiToS = Milano Torino staging system.

and electro-oculography (EOG) were also acquired in order to remove physiological artefacts. Finally, after applying an anti-aliasing filter, the data were sampled at 1024 Hz.

2.4. Preprocessing

Data preprocessing was performed similarly to Liparoti et al. (Liparoti et al., 2021). Briefly, using the Fieldtrip toolbox in MATLAB the MEG data were filtered in the 0.5–48 Hz band using a 4th-order Butterworth IIR band-pass filter. Principal component analysis (PCA) was carried out to reduce environmental noise. Then, we performed Independent Component Analysis (ICA) in order to remove from the MEG data physiological artefacts from the ECG (on average one component for each subject was removed) and from EOG (zero component per participant, rarely one) (Sorrentino et al., 2018). We performed the entire procedure again, as already described, but this time we used an automated cleaning algorithm instead of the expert rater to clean the signals. Details on the applied clinical algorithm can be found at (Sorriso et al., 2019).

2.5. Source reconstruction

MEG data were co-registered with the native MRI of each subject. We obtained the time series of the 90 regions of interest (ROIs) according to the Automated Anatomical Labelling (AAL) atlas (Gong et al., 2009). To this end, we used the volume conduction model proposed by Nolte (Nolte, 2003) and the Linearly Constrained Minimum Variance (LCMV) (Van Veen et al., 1997) beamformer algorithm based on the native MRIs. The time series were then filtered in the five classical frequency bands: (i.e., delta (0.5–4 Hz), theta (4–8 Hz), alpha (8–13 Hz), beta (13–30 Hz), and gamma (30–48 Hz).

2.6. Synchrony estimation

To estimate the synchronisation between brain regions we used the PLM, a measure based on the spectrum of the interferometric signal obtained from any pair of brain regions, which is insensitive to volume conduction (Baselice et al., 2018), and ranges from 0 (no synchronisation) to 1 (synchronisation). Hence, using the two separate recordings, we obtained two FCs (per frequency band) that we named test and re-test.

2.7. Fingerprint analysis

In order to characterize individual brain connectivities, we adopted an approach based on the FCs (Fig. 1). Firstly, we built n frequency-specific identifiability matrices (IM) for each group, performing Pearson's correlation between the test and the re-test FCs. The IM have subjects on rows and columns, which refer to the test FCs and re-test FCs, respectively (Amico and Goñi, 2018). Each frequency-specific matrix contained the following information: each element of the main diagonal represents the similarity between two FCs of the same individual, defined as (*I-self*); each off-diagonal element represents the similarity across two FCs belonging to two different individuals; averaging all the off-diagonal elements on a row and column corresponding to a specific subject conveys the similarity of that individual with the whole group, defined as *I-others;* then, computing the difference between the *I-self* and the *I-others* we obtained the differential identifiability (*I-diff*). This score

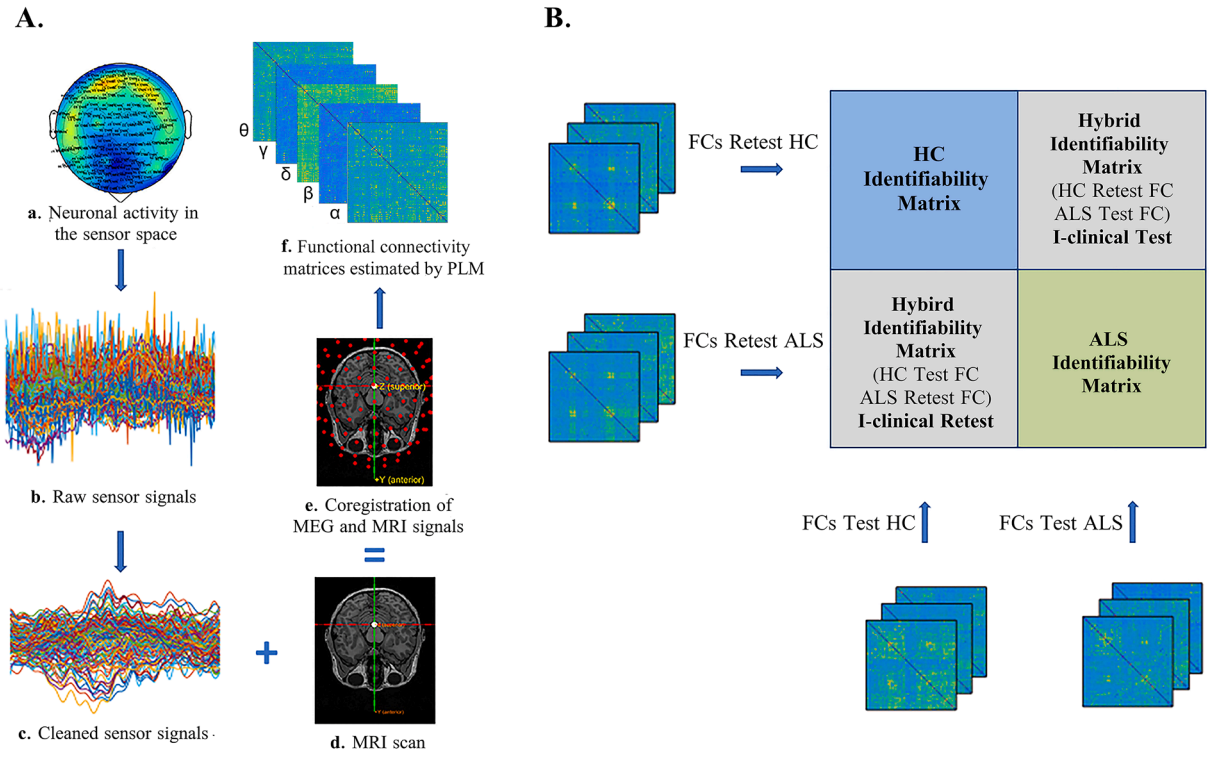

Fig. 1. Pipeline analysis and clinical connectome fingerprint application. (A) a: the neuronal activity was recorded using a magnetoencephalography (MEG) composed by 154 sensors; **b:** raw MEG signals including noise, and cardiac and blinking artefacts; **c:** MEG signals after removing noise and physiological artefacts; **d:** magnetic resonance image (MRI) of a subject; **e:** coregistration of MEG and MRI signals to obtain the source reconstruction (beamforming); **f:** functional connectivity matrix (one for each frequency band) estimated using the phase linearity measurement (PLM). Each matrix displays on both rows and columns the 90 ROIs **(B)** The blue and the green blocks represents the two identifiability matrices of healthy controls (HC) and Amyotrophic Lateral Sclerosis (ALS) patients, respectively obtained by correlating the test and re-test individual functional connectomes, in each group separately. Crossing the FCs test of the HC with the FCs retest of the ALS and vice-versa, we obtained two hybrid identifiability matrices, that allowed us to calculate the I-clinical value of each patient (expressing how much an ALS patient is similar to the HC group). (For interpretation of the references to colour in this figure legend, the reader is referred to the web version of this article.)

provides an estimation of the fingerprint level of each subject within a specific brain data set (Amico and Goñi, 2018).

In this study we used an extension of the identifiability approach by crossing the ALS patients and the control group test and re-test FCs to obtain the I-clinical score which assesses how much each patient was similar to healthy controls (Sorrentino et al., 2021b). To this end, we built two hybrid matrices: the first one by correlating the controls' tests with the patients' re-tests; the second one correlating the controls' re-tests and the patients' test FCs. In particular, the I-clinical (test) represents the mean similarity over the FCs of a given patient in the test session with the FCs of every healthy control in the retest session while the I-clinical (retest) represents the opposite case (i.e., the mean similarity between the FCs of a specific patient in the retest session, with the FCs of every healthy control in the test session). Finally, the I-clinical was obtained by averaging the I-clinical (test) with the I-clinical (retest) (Sorrentino et al., 2021b).

2.8. Edge-wise fingerprinting

To test the edgewise reliability of individual connectomes, we used the one-way random effects intra-class correlation coefficient (ICC) (Koch, 2004, McGraw and Wong, 1996). The ICC is a statistical measurement used to assess the separability between elements of the different groups (Amico and Goñi, 2018). In the case of the functional connectomes, the edges (i.e., the link between two nodes) with a high ICC value are likely those that contribute the most to identifiability. We evaluated brain fingerprints (Finn et al., 2015) by sequentially adding 50 edges, starting from those that contribute the most to identifiability to those that contribute the least. At each iteration, we calculated the success rate (SR), obtained as the percentage of subjects that were identified with respect to each subject of the same group. Thus, we obtained a distribution of SR values averaged for each group. To test the reliability of our approach, a null model analysis was performed by adding the edges in random order, one hundred times at each step, to verify that the distribution curve of the SR was statistically meaningful. However, it must be highlighted that the SR estimation might be slightly inflated with respect to the null model, since the edge order is influenced by the ICC scores, which are based on all the analysed subjects. For generalisation purposes it would be advised to perform this analysis partitioning the data if the sample size allows it.

2.9. Fingerprint clinical prediction

We tested the hypothesis that the *I-clinical* could predict the clinical impairment of the patient. Thus, we built a multilinear regression model to predict the ALSFRS-r, the King's and the MiToS scores based on the *I-clinical* scores (in the alpha band), alongside with four other predictors: age, sex, education level and duration of disease. Multicollinearity, linearity and normality were assessed through the variance inflation factor (VIF) (Craney and Surles, 2002), the Durbin-Watson test and the Kolmogorov-Smirnov test, respectively, while homoscedasticity has been checked visually. To strengthen the reliability of our approach we performed the leave-one-out-cross validation (LOOCV) (Varoquaux et al., 2017). Specifically, we built n multilinear models (where n is the number of subjects), each time excluding a different subject from the analysis in order to verify the ability of the model to predict the ALSFRS-r, the King's and the MiToS score of the excluded subject.

2.10. Further validation

To investigate the reliability of the information contained in the FCs of our patients, we also tested their relationship with the clinical condition using the connectome-based predictive modelling (CPM) framework (Shen et al., 2017). In brief, this is a technique that selects relevant edges based on the presence of a relationship with behaviour or, as in our case, the clinical condition of patients (assessed through the ALSFRS-r, the King's and the MiToS scores). The analysis was performed within the LOOCV framework and the predicted results of the CPM model were compared with the actual ones through Spearman's correlation test. Please refer to (Shen et al., 2017) for further technical details. Finally, in order to retrieve information concerning specific regions, we summed the number of times each edge of the FCs was above threshold in the CPM pipeline, obtaining a matrix of edge occurrences, over which we computed the nodal strength. Observing the distribution of those occurrences, we selected the ones falling above the 95% confidence interval threshold.

2.11. Statistical analysis

Statistical analysis was carried out in MATLAB 2021a. I-*self,* *I-others* and *I-diff* values were compared between the two groups through a permutation test, shuffling the data 10,000 times. At each iteration, the absolute difference between the means of the two randomly generated groups was observed, generating a null distribution of differences. Then, the observed difference between patients and controls was compared to the random distribution to obtain a statistical significance. The possible relationship between the *I-clinical* score and the clinical condition of the patients was investigated through Spearman's correlation. The results were corrected across frequency bands using the False Discovery Rate (FDR) method (Benjamini and Hochberg, 1995). Significance level was set at p-value < 0.05 after correction.

3. Results

3.1. Fingerprint analysis

As a whole, we observed a reduction in ALS patients' identifiability compared to the HC group in the alpha band (Fig. 2). Specifically, we found a statistically significant difference between the *I-self* (pFDR $=$ 0.0249) and the *I-others* (pFDR $= 0.0003$) of the patients as compared to that of the controls. Moreover, to corroborate the interpretation of our results, we compared the I-others (how much each subject differs from the other subjects) of the HC with the I-clinical (how much each patient is similar to the control group) of the ALS. Even in this case, we found a statistically significant difference between the HC I-others and the I-clinical of the patients (pFDR $= 0.0001$). We did not find any statistically significant difference between the *I-diff* values between the HC and the ALS groups in any of the five frequency bands. The results are confirmed when using an automated cleaning algorithm (Sorriso et al., 2019), as shown in the supplementary materials. Specifically, we still observed a drop in the identifiability of the ALS group compared to the HC group in the alpha band. The significant difference is confirmed with respect to *I-others* while a trend is present for the *I-self* (see supplementary materials 1).

3.2. Edge-based identifiability

We observed, in the alpha band, that the contribution of brain regions to identifiability was slightly reduced in patients as compared to healthy subjects. In fact, the control group presented higher values in the ICC matrices (Fig. 3A) as compared to that of the ALS patients revealing a greater stability of the connectivity between the edges. Thus, the contribution to the fingerprint is derived from fewer brain regions in the patients compared to controls, as shown in Fig. 3B. Furthermore, calculating the absolute difference of the nodal strength of the ICC matrices, we highlighted four brain regions whose stability of the connectivity differed significantly. In particular, the ICC nodal strength of the ALS group was lower than in HC group in the right parietal inferior lobule, the right cuneus, the right parahippocampal gyrus, and the left amygdala.

Thereafter, we analysed the SR values distribution obtained performing the fingerprint analysis adding 50 edges at a time, from the most

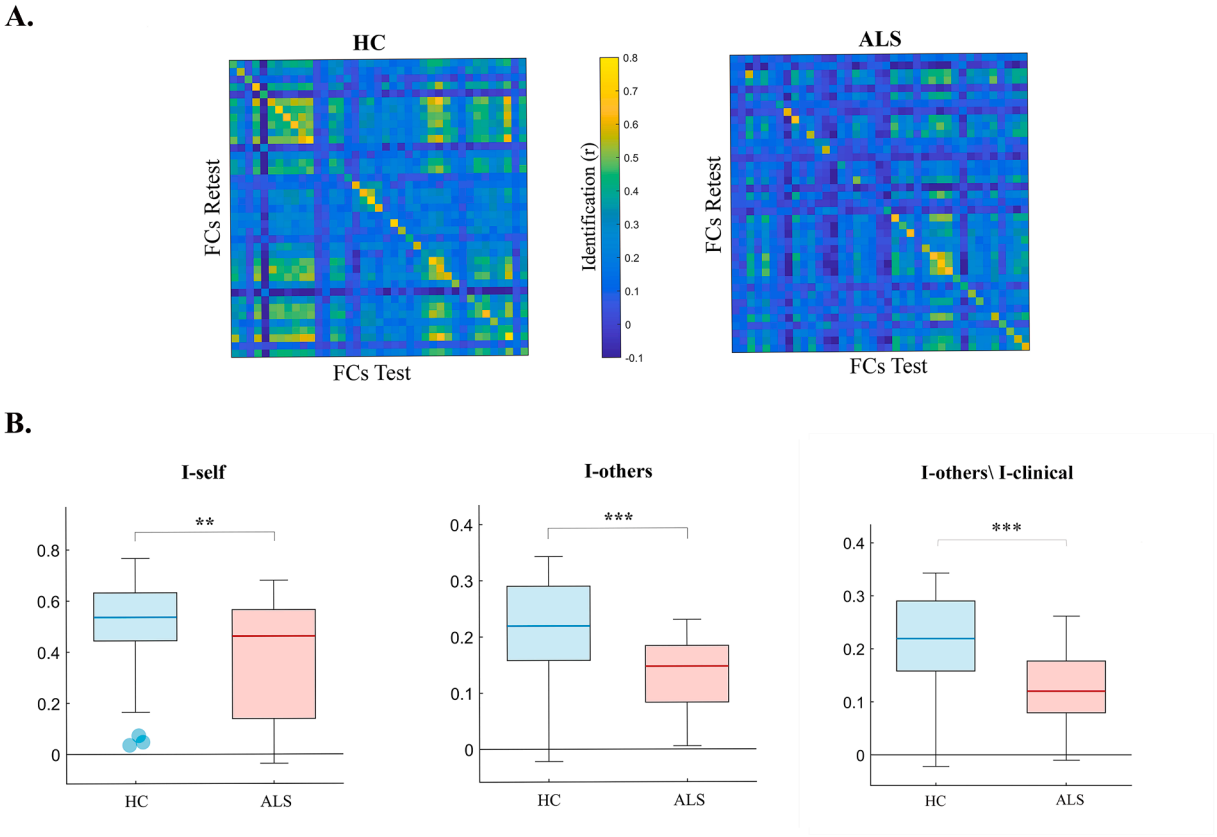

Fig. 2. Identifiability matrices and fingerprint features comparison. (A). Identifiability matrices comparison in the alpha band. The main diagonal is representative of the *I-self* while the *I-others* is represented by all the elements outside the main diagonal. The main diagonal of the healthy controls' (HC) identifiability matrix (IM) is more visible as compared to the amyotrophic lateral sclerosis patients's (ALS) one, revealing a reduction in self similarity (i.e lower I-self values) of the ALS compared to the HC. **(B)** Fingerprint features comparison in the alpha band. HC displays higher values of both I-self and I-others as compared to ALS patients. The right panel shows the comparison between the HC *I-others* and the *I-clinical* of the patients. Even in this case, HC displays higher values of *I-others* compared to the *I-clinical* of the patients confirming the drop of identifiability. FCs = functional connectomes. significant p value is indicated with **($p < 0.01$) and *** ($p < 0.001$).

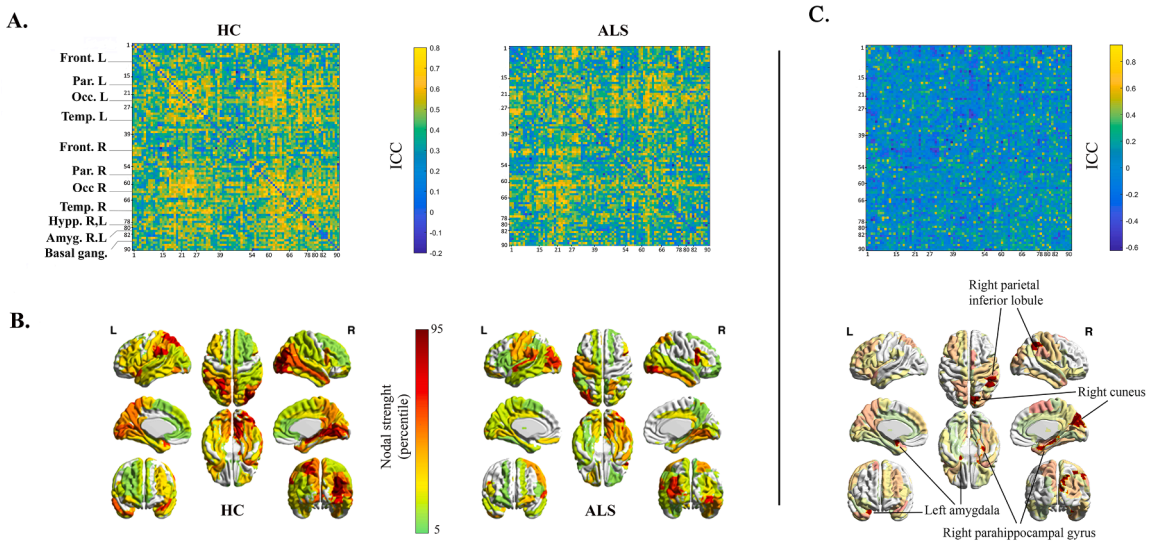

Fig. 3. Edge contribution to connectomes' identifiability. (A) The intra-class-correlation (ICC) matrices show the edges contribution to the identifiability in the alpha band. We can observe a drop in ICC in the amyotrophic lateral sclerosis (ALS) as compared to the healthy controls (HC). This means that in the patients there are less reliable brain regions that contribute to self-identification. The rank of the 90 ROIs is displayed in the left panel. **(B)** The same results are represented as brain renders, showing the nodal strength of the most reliable edges. (from 5th to 95th percentile). The nodal strength values are obtained by summing the elements of both rows and columns of the lower part of the ICC matrices. **(C)** Difference between the HC ad ALS ICC matrices, with the consequent brain renders in which we highlighted the brain regions whose nodal strength significantly differed between the two groups. The healthy controls showed higher nodal strength values in all four brain regions.

to the least contributing ones, according to the ICC matrices. After a few hundreds of edges (~400), the HC group reached 95% identification success, that then remained stable. With respect to the null model, SR values of the healthy controls did not diverge significantly. The ALS group needed more edges (with respect to the HC group) in order to reach its identification plateau, which settled at 85% starting from ~ 700 edges. For the ALS group, the ICC ordered identification was similar to the null model (Fig. 4).

3.3. Multilinear regression model

Then, we computed the *I-clinical* score of each ALS patient in the alpha band. We added these values, which represent the similarity of each patient to the healthy group into a multilinear regression model to test the capacity of the *I-clinical* to predict the clinical condition as assessed by the ALSFRS-r, the King's and the MiToS clinical scales (Fig. 5). Besides the *I-clinical*, the predictive model was composed by four other predictors: age, sex, education level and disease duration. We found that the *I-clinical* significantly increases the predictive power of the model for the ALSFRS-r ($F(5.33) = 3.95$; $R2 = 0.38$; $p = 0.0006$; $\beta = 32.8$), the King's ($F(5.33) = 8.36$; $R2 = 0.56$; $p = 0.0001$; $\beta = -7.40$) and the MiToS ($F(5.33) = 7.12$; $R2 = 0.52$; $p = 0.0025$; $\beta = -4.9$) scores. As expected, the disease duration also significantly contributed to the prediction of the ALSFRS-r ($p = 0.0132$; $\beta = -0.0484$), the King's ($p = 0.0015$; $\beta = 0.0069$) and the MiToS ($p = 0.0001$; $\beta = 0.0077$) while no significant contribution of age, education and gender was observed. The results are confirmed when using a different cleaning algorithm (Sorriso et al., 2019). In particular, the predictive power of the I-clinical is confirmed with respect to the King's scale, while a trend is present for the ALSFRS-r and the MiToS scales (see supplementary materials 2).

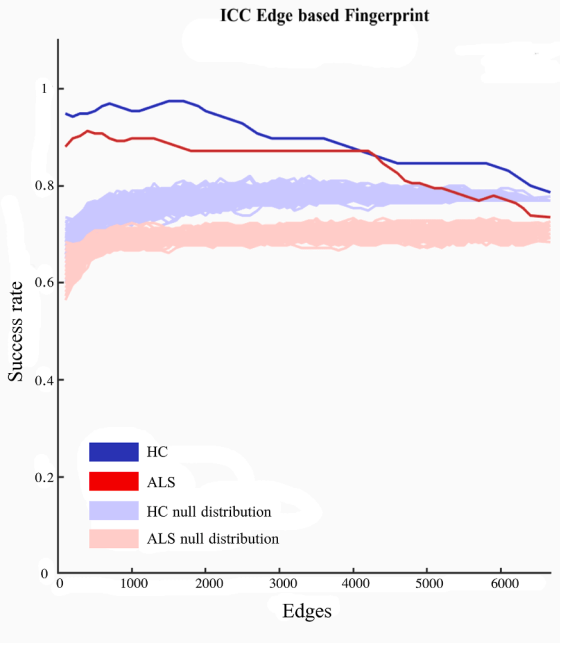

Fig. 4. Iterative model of edgewise subjects' identification. The success rate (SR) of healthy controls (HC, blue line) and Amyotrophic Lateral Sclerosis patients (ALS, red line) were obtained performing the fingerprint analysis by adding 50 edges at a time from those contributing the least to identifiability to those which contributed the most, according to the intraclass correlation (ICC) values. The light blue line and the light red line were representative of the null distributions (obtained by adding the edges in a random order, one hundred times at each step) for the HC and ALS patients respectively. The observed SR values are higher values as compared to the null model distributions for both patients and HC. (For interpretation of the references to colour in this figure legend, the reader is referred to the web version of this article.)

3.4. Fingerprint and disease clinical staging

We explored the possibility of a linear relationship between the *I-clinical* and the three clinical scores through the Spearman's correlation in the alpha band. As one can see in Fig. 6, we found significant correlations between the I-clinical and both the King's and the MiToS disease staging system. Specifically, we found a significant negative correlation, after FDR correction, between the *I-clinical* and the King's ($r = -0.6041$; $pFDR = 0.0003$) disease staging system and between the *I-clinical* and the MiToS ($r = -0.4953$; $pFDR = 0.0040$) disease staging system. We did not find any significant correlation between the *I-clinical* and the ALSFRS-r.

3.5. CPM analysis

The CPM prediction for the King's scale was significantly correlated with the observed individual scores ($r = 0.46$, $p = 0.0035$), even after a permutation testing in which the clinical scores were shuffled among patients ($p = 0.0131$). There was no significant correlation for the prediction of the ALSFRS-r ($r = 0.175$, $p = 0.286$) and the MiToS ($r = 0.302$, $p = 0.062$) scores. Furthermore, calculating the nodal strength of the main edges involved in the King's scale prediction, we retrieved four specifically relevant regions: the left occipital superior gyrus, the left calcarine cortex, the right occipital gyrus, and the right lingual gyrus.

4. Discussion

In the present study, we applied the clinical connectome fingerprint (CCF) to compare subject-specific connectomes from thirty-nine ALS patients to those of thirty-nine healthy matched controls. Our hypothesis was that the widespread brain connectivity alterations of ALS patients would make the FCs less recognisable with respect to the healthy controls. Furthermore, we tested the hypothesis that such a reduced identifiability might be associated with the individual clinical picture. Hence, based on source-reconstructed MEG data, we reconstructed the functional connectomes using the PLM as a synchronisation measure. Then, we investigated the identifiability features in ALS patients and healthy individuals. The comparison between the identifiability matrix of the patients and of the healthy subjects showed a drop of identifiability in the patients as compared to the matched controls in the alpha band. Specifically, we found that the patients' *I-self* and *I-others* were lower than those of the control, while there was no statistically significant difference between the *I-diff* of the two groups. The difference in identifiability between the two groups has also been confirmed by the difference between the *I-others* of the controls and the *I-clinical* of the patients. As previously suggested, the loss of identifiability might be ascribed to the reorganisation of the large-scale networks occurring in ALS, which makes the functional connectomes of the patients less similar to themselves (Sorrentino et al., 2021b). This could be largely due to the alteration of communication patterns in the diseased brain (Proudfoot et al., 2017). Even beyond the resting-state, a MEG study (Proudfoot et al., 2017) showed that ALS led to a reduction in synchronisation during the execution of a motor tasks. Alterations in synchronisability might be related to the brain operating in a suboptimal dynamical regime which does not support efficient and flexible communication between brain regions (Sorrentino et al., 2021a). This might in turn manifest itself as a more stereotyped, less identifiable brain activity.

Interestingly, our results were specific to the alpha band. The presence of connectivity alterations in the alpha band in ALS has also been pointed out in other studies. For example, Iyer et al., (Iyer et al., 2015) showed increased assortativity in the alpha-band in ALS patients as compared to controls, as well as higher clustering coefficient values based on Partial Directed connectivity (PCD). Similarly, an EEG study conducted by Perez Ortiz et al. (Perez-Ortiz et al., 2021) displayed the presence of connectivity alterations (in the sense of reduced

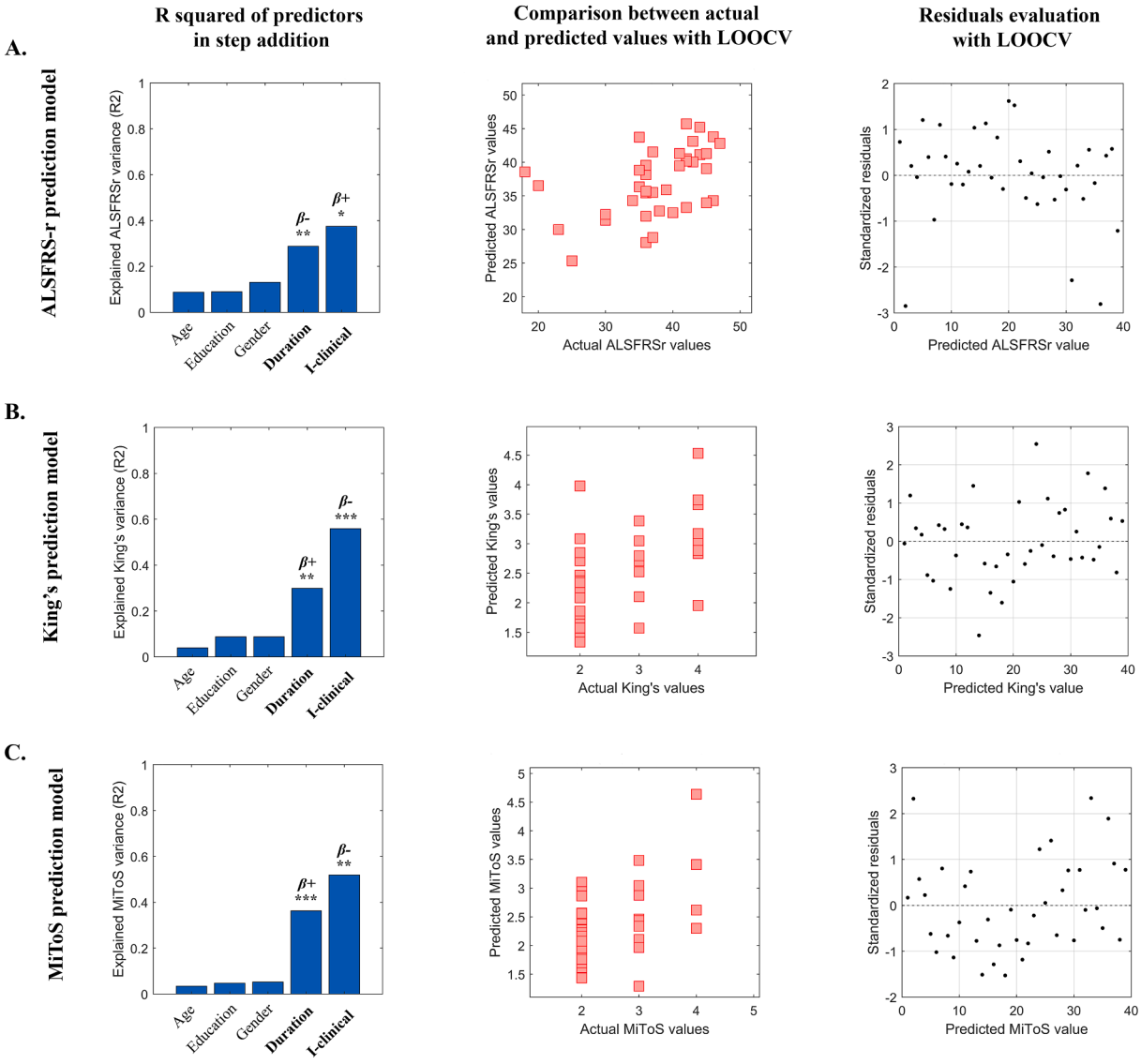

Fig. 5. Motor impairment prediction in the alpha band. A multilinear regression model with leave-one-out cross validation (LOOCV) was performed to test the capacity of the "clinical fingerprint" (i.e., the I-clinical score) to predict the motor impairment in amyotrophic lateral sclerosis (ALS) patients. The predictive models of the ALS functional rating scale revised (ALSFRS-r) **(A)**, the King's disease staging system **(B)** and the Milano Torino staging system (MiTos) are represented on the rows**.** The left column reports the explained variance obtained by adding the five predictors (age, education, gender, duration of disease and I-clinical in alpha band). The significant predictors are highlighted in bold while the positive and negative coefficients are indicated with β+/β-, respectively. The significant p value is indicated with * ($p < 0.05$) ** ($p < 0.01$) and *** ($p < 0.001$). The central column shows the comparison between the observed and the predicted values of the response variable, validated through LOOCV for **A, B** and **C,** respectively. The right column represents the distribution of the standardised residuals (i.e., standardisation of the difference between observed and predicted values).

synchronisation) in the alpha band in ALS patients during the execution of cognitive tasks. According to Fraschini et al. (Fraschini et al., 2018) ALS patients showed reduced brain functional connectivity compared to healthy subjects, which was linked to different synchrony patterns in the alpha band. Nevertheless, alterations in functional connectivity have been reported in all frequency bands (Dukic et al., 2022; Nasseroleslami et al., 2019; Proudfoot et al., 2017). Our is the first study which explores the individual connectome features in ALS using the CCF approach. Hence, further investigations are warranted to establish whether the identifiability alterations in ALS patients are frequency band specific.

Notably, head movements do not seem to affect the reliability of our results since the comparison between the displacement of the head in the helmet at the beginning of each segment of acquisition did not differ significantly between groups. However, the head position throughout the acquisition was not tracked, and this does not allow to fully account for the effects of potentially different movement patterns. Furthermore, we have also replicated the analysis using a different cleaning algorithm, which again is comforting with respect to the resilience of the analysis to artefacts (see Supplementary Material 1).

Furthermore, we performed an ICC-based analysis to assess which brain regions mostly contribute to identifiability, assuming that the greater the ICC value, the greater the contribution of a given edge to identifiability (Amico and Goñi, 2018). As we expected, the reliability of the connectivity between different brain regions was reduced in patients as compared to healthy subjects. We hypothesised that this result might be ascribed to the widespread functional alterations which contributed to determine the loss of stable subject-specific connectivity in ALS patients. Several hypotheses have been put forward concerning the occurrence of these alterations. According to Poujois et al., this process might be caused by a reorganisation of both the motor and extra-motor

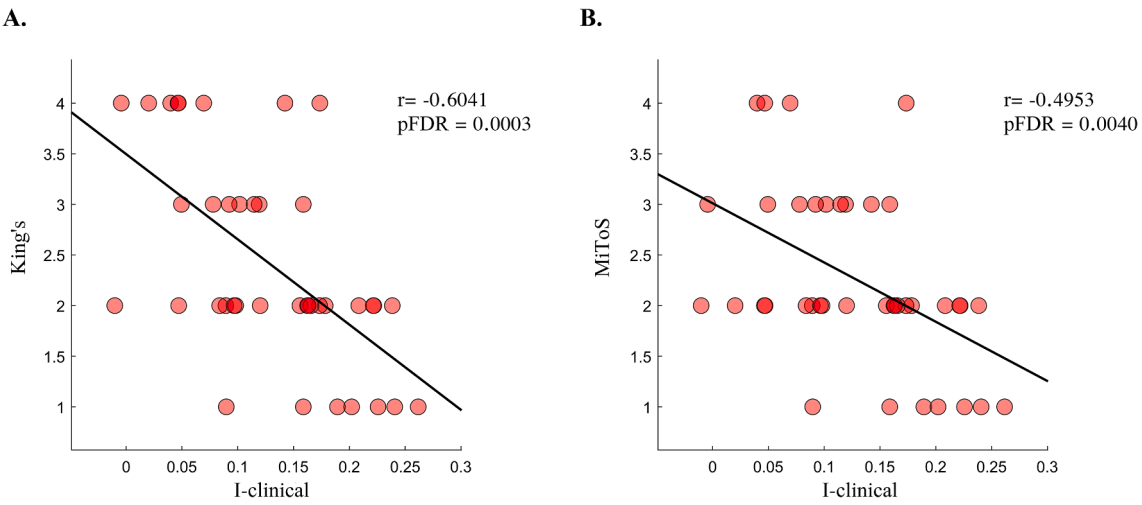

Fig. 6. Correlation between motor impairment and I-clinical. (A) Spearman's correlation between the King's disease staging system and the clinical identifiability (i.e., the I-clinical). The negative correlation coefficient indicates that as the I-clinical scores increase, the King's scores decrease and, thus, the ALS patients show better motor functions. **(B)** Negative correlation between the Milano-Torino staging system (MiToS) and the I-clinical. Higher MiToS scores (i.e., worse motor condition) correspond to lower I-clinical scores and vice versa.

regions through neural plasticity modulations (Poujois et al., 2013), which would occurs as a compensatory mechanism to ALS neurodegeneration (Trojsi et al., 2012). In another study proposed by Turner et al., it has been shown that brain functional alterations in ALS could partly result from the loss of inhibitory interneurons (Turner and Kiernan, 2012). In this regard, note that a reduction in GABAergic inhibition is responsible for the cortical hyperexcitability typical of ALS (Kiernan and Petri, 2012) and that, more importantly, the reduced cortical inhibition, ascribed to the loss of GABAergic interneurons, might lead to increased functional connectivity (Douaud et al., 2011). Furthermore, comparing the nodal strength of the edge reliability, we observed reduced stability in four regions in the ALS group. On the one hand, we found the cuneus and the parietal inferior lobule, which are known to be involved in sensory information processing. Moreover, those regions are part of the so-called "dorsal stream" which, according to the two-streams theory, is associated with the individual spatial awareness and the coordination of the body in space (Kravitz et al., 2011; Micheletti et al., 2021). On the other hand, reduced stability was also observed in the amygdala and the parahippocampal, which may be in line with the converging evidence pointing at the widespread nature of ALS. Indeed, several works reported an association between the altered functioning of those regions and cognitive dysfunctions in ALS (Chipika et al., 2020; Kawashima et al., 2001).

Following the information given by the ICC matrices, we investigated the contribution of the edges in identifying the FCs of both groups. As shown in Fig. 4, a few hundred edges were sufficient to obtain optimal subject recognition. Furthermore, increasing the number of the edges did not improve identification and, rather, reduced it. We hypothesised that this finding is a consequence of the fact that subject-specific patterns are encoded within a restricted number of connections. Conversely, including more information (i.e., more edges to the analysis) we might be more likely to include patterns that are common among different individuals (Gratton et al., 2018) and, hence, do not contribute to subject identification. Furthermore, the reduction in edge-based identifiability was more prominent in patients than in controls. This is in accordance with our results on the reliability of the connections, which showed fewer stable links in patients. However, we should point out some limitations on this approach. First, the actual identification of the subjects was enhanced with respect to the null model, since the ICC scores we used to order the edges were calculated keeping into consideration all the subjects of each group. Hence, the generalizability of this analysis remains to be explored. As an example, larger samples could allow partitioning the dataset.

Finally, we explored the relationship between the CCF features and the clinical assessment of the disease and its rate progression. Previous evidence suggested that alterations in functional connectivity can be considered as a marker of disease progression (Dubbelink et al., 2013), and that they can be related to the rate of disability (Fraschini et al., 2016). Our results are in agreement with the above findings and might help to inform the management of the disease. Indeed, our analysis highlighted an association between the subject-specific clinical identification (i.e., *I-clinical*) and the motor impairment evaluation. Specifically, the multilinear regression model that we built pointed out that, among all predictors (age, sex, education level and duration of disease), the *I-clinical*, together with the duration of the disease, was able to significantly predict the ALSFRS-r, the King's disease staging system and the MiToS scores. Furthermore, the generalisation and prediction capacity of our models was assessed using the LOOCV. With regard to the disease duration, it is obvious that such a relation would exist, since ALS is a progressive neurodegenerative disease. However, the *I-clinical* adds novel information which improves the clinical predictions, connecting the clinical picture to brain identifiability. This relationship was strengthened by the negative correlation between the I-clinical and the King's and the MiToS scores. Indeed, patients with higher I-clinical scores were more similar to the control group and, accordingly, their motor functions were less compromised. We have also repeated the correlation analysis only taking into account the reliable edges (as opposed to considering all the edges) but retrieved no significant correlation in this case. This might be due to the reduced statistical power, or to the fact that such choice of edges alone does not carry enough information to directly relate to the clinical picture, or yet that this relationship is masked by confounders. Analyses with larger samples and using different methodologies might help disentangling these possibilities.

Finally, the CPM analysis reinforced the general expectation that clinically relevant information was present in the FCs of our patients, although predictions were not confirmed for all three clinical scales, but only for the King's scale. One can speculate that the differences between the CPM and the I-clinical may lie in the fact that the latter is more subject-specific, highlighting the degrees of change of a single subject with respect to the healthy population, while the first offers an overview related to the overall disease impairment. In particular, the CPM of the King's scale pointed out brain regions clustered within the right and left occipital lobes. Interestingly, the CMP analysis highlighted the

involvement of the occipital lobes, which is in accordance with our findings regarding the differences in the ICC between ALS patients and HC (see Fig. 3, panel C). Converging lines of evidence assessed functional connectivity alterations in occipital regions in ALS (Loewe et al., 2017; Zhang et al., 2017). These alterations were associated to the onset of clinical symptoms, such as a reduced response to visual stimulations, as well as to structural damage characterised by demyelination of sensory fibres (Lulé et al., 2010) or by grey matter atrophy in the occipital lobes (Bakulin et al., 2019).

5. Conclusions

In conclusion, in the present paper, we applied the CCF framework to ALS patients, to test its reliability in a clinical setting which is predominantly characterised by motor impairment. In accordance to our hypothesis, ALS patients showed reduced identifiability as compared to healthy subjects. Moreover, the connectomes of less-severely impaired patients showed greater similarity to the connectomes of the healthy individuals. Finally, the predictive power of the clinical fingerprint to predict the individual rate of disease progression may represent a promising tool in ALS clinical management. Thanks to the subject-specific characteristic of this approach, we hope that further exploration might lead to tailored diagnostic and therapeutic strategies.

6. Data and code availability statement

The data supporting the findings of this study are available from the corresponding author upon reasonable request, for purpose of replication. The data are not publicly available due to the clinical nature of the cohort under study. The code (MATLAB) used for this analysis is available at the following link: https://github.com/eamico/Clinical_fingerprinting.

Funding

GS acknowledges financial support for University of Naples "Parthenope" within the project "Bando Ricerca Competitiva 2017" (D.R 289/2017).

Declaration of Competing Interest

The authors declare that they have no known competing financial interests or personal relationships that could have appeared to influence the work reported in this paper.

Acknowledgments

We would like to thank Silvia Lombardini for the english revision of the manuscript.

Appendix A. Supplementary data

Supplementary data to this article can be found online at https://doi.org/10.1016/j.nicl.2022.103095.

References

Agosta, F., Ferraro, P.M., Riva, N., Spinelli, E.G., Chiò, A., Canu, E., Valsasina, P., Lunetta, C., Iannaccone, S., Copetti, M., 2016. Structural brain correlates of cognitive and behavioral impairment in MND. Hum. Brain Mapp. 37, 1614–1626.

Amico, E., Goñi, J., 2018. The quest for identifiability in human functional connectomes. Sci. Rep. 8, 1–14.

Bakulin, I.S., Konovalov, R.N., Krotenkova, M.V., Suponeva, N.A., Zakharova, M.N., 2019. Voxel-based morphometry in amyotrophic lateral sclerosis. J. Radiol. Nucl. Med. 99, 287–294. https://doi.org/10.20862/0042-4676-2018-99-6-287-294.

Balendra, R., Al Khleifat, A., Fang, T., Al-Chalabi, A., 2019. A standard operating procedure for King's ALS clinical staging. Amyotroph. Lateral Scler. Front. Degener. 20, 159–164.

Baselice, F., Sorriso, A., Rucco, R., Sorrentino, P., 2018. Phase linearity measurement: A novel index for brain functional connectivity. IEEE Trans. Med. Imaging 38, 873–882.

Benjamini, Y., Hochberg, Y., 1995. Controlling the false discovery rate: a practical and powerful approach to multiple testing. J. R. Stat. Soc. Ser. B Methodol. 57, 289–300.

Bersano, E., Sarnelli, M.F., Solara, V., Iazzolino, B., Peotta, L., De Marchi, F., Facchin, A., Moglia, C., Canosa, A., Calvo, A., 2020. Decline of cognitive and behavioral functions in amyotrophic lateral sclerosis: a longitudinal study. Amyotroph. Lateral Scler. Front. Degener. 21, 373–379.

Brooks, B.R., 1994. El Escorial world federation of neurology criteria for the diagnosis of amyotrophic lateral sclerosis. Subcommittee on motor neuron diseases/amyotrophic lateral sclerosis of the world federation of neurology research group on neuromuscular diseases and th. J. Neurol. Sci. 124, 96–107.

Cedarbaum, J.M., Stambler, N., Malta, E., Fuller, C., Hilt, D., Thurmond, B., Nakanishi, A., Group, B.A.S., Group, 1A complete listing of the BDNF Study, 1999. The ALSFRS-R: a revised ALS functional rating scale that incorporates assessments of respiratory function. J. Neurol. Sci. 169, 13–21.

Chipika, R.H., Christidi, F., Finegan, E., Li Hi Shing, S., McKenna, M.C., Chang, K.M., Karavasilis, E., Doherty, M.A., Hengeveld, J.C., Vajda, A., Pender, N., Hutchinson, S., Donaghy, C., McLaughlin, R.L., Hardiman, O., Bede, P., 2020. Amygdala pathology in amyotrophic lateral sclerosis and primary lateral sclerosis. J. Neurol. Sci. 417, 117039 https://doi.org/10.1016/j.jns.2020.117039.

Craney, T.A., Surles, J.G., 2002. Model-dependent variance inflation factor cutoff values. Quality Eng. 14, 391–403. https://doi.org/10.1081/QEN-120001878.

Douaud, G., Filippini, N., Knight, S., Talbot, K., Turner, M.R., 2011. Integration of structural and functional magnetic resonance imaging in amyotrophic lateral sclerosis. Brain 134, 3470–3479.

Dubbelink, K.T.E.O., Stoffers, D., Deijen, J.B., Twisk, J.W.R., Stam, C.J., Hillebrand, A., Berendse, H.W., 2013. Resting-state functional connectivity as a marker of disease progression in Parkinson's disease: a longitudinal MEG study. NeuroImage Clin. 2, 612–619.

Dukic, S., McMackin, R., Costello, E., Metzger, M., Buxo, T., Fasano, A., Chipika, R., Pinto-Grau, M., Schuster, C., Hammond, M., Heverin, M., Coffey, A., Broderick, M., Iyer, P.M., Mohr, K., Gavin, B., McLaughlin, R., Pender, N., Bede, P., Muthuraman, M., van den Berg, L.H., Hardiman, O., Nasseroleslami, B., 2022. Resting-state EEG reveals four subphenotypes of amyotrophic lateral sclerosis. Brain 145, 621–631. https://doi.org/10.1093/brain/awab322.

Fang, T., Al Khleifat, A., Stahl, D.R., Lazo La Torre, C., Murphy, C., LicalS, U.-M., Young, C., Shaw, P.J., Leigh, P.N., Al-Chalabi, A., 2017. Comparison of the King's and MiToS staging systems for ALS. Amyotroph. Lateral Scler. Front. Degener. 18, 227–232.

Finn, E.S., Shen, X., Scheinost, D., Rosenberg, M.D., Huang, J., Chun, M.M., Papademetris, X., Constable, R.T., 2015. Functional connectome fingerprinting: identifying individuals using patterns of brain connectivity. Nat. Neurosci. 18, 1664–1671.

Fraschini, M., Demuru, M., Hillebrand, A., Cuccu, L., Porcu, S., Di Stefano, F., Puligheddu, M., Floris, G., Borghero, G., Marrosu, F., 2016. EEG functional network topology is associated with disability in patients with amyotrophic lateral sclerosis. Sci. Rep. 6, 1–7.

Fraschini, M., Lai, M., Demuru, M., Puligheddu, M., Floris, G., Borghero, G., Marrosu, F., 2018. Functional brain connectivity analysis in amyotrophic lateral sclerosis: an EEG source-space study. Biomed. Phys. Eng. Express 4, 37004.

Geser, F., Brandmeir, N.J., Kwong, L.K., Martinez-Lage, M., Elman, L., McCluskey, L., Xie, S.X., Lee, V.M.-Y., Trojanowski, J.Q., 2008. Evidence of multisystem disorder in whole-brain map of pathological TDP-43 in amyotrophic lateral sclerosis. Arch. Neurol. 65, 636–641.

Goldstein, L.H., Abrahams, S., 2013. Changes in cognition and behaviour in amyotrophic lateral sclerosis: nature of impairment and implications for assessment. Lancet Neurol. 12, 368–380.

Gong, G., He, Y., Concha, L., Lebel, C., Gross, D.W., Evans, A.C., Beaulieu, C., 2009. Mapping anatomical connectivity patterns of human cerebral cortex using in vivo diffusion tensor imaging tractography. Cereb. Cortex 19, 524–536.

Gratton, C., Laumann, T.O., Nielsen, A.N., Greene, D.J., Gordon, E.M., Gilmore, A.W., Nelson, S.M., Coalson, R.S., Snyder, A.Z., Schlaggar, B.L., Dosenbach, N.U.F., Petersen, S.E., 2018. Functional brain networks are dominated by stable group and individual factors, not cognitive or daily variation. Neuron 98, 439–452.e5. https://doi.org/10.1016/j.neuron.2018.03.035.

Iyer, P.M., Egan, C., Pinto-Grau, M., Burke, T., Elamin, M., Nasseroleslami, B., Pender, N., Lalor, E.C., Hardiman, O., 2015. Functional connectivity changes in resting-state EEG as potential biomarker for amyotrophic lateral sclerosis. PLoS One 10, e0128682.

Iturria-Medina, Y., Evans, A.C., 2015. On the central role of brain connectivity in neurodegenerative disease progression. Front. Aging Neurosci. 7, 90.

Kiernan, M.C., Petri, S., 2012. Hyperexcitability and amyotrophic lateral sclerosis. Neurology.

Koch, G.G., 2004. Intraclass correlation coefficient. Encycl. Stat. Sci.

Liparoti, M., Troisi Lopez, E., Sarno, L., Rucco, R., Minino, R., Pesoli, M., Perruolo, G., Formisano, P., Lucidi, F., Sorrentino, G., Sorrentino, P., 2021. Functional brain network topology across the menstrual cycle is estradiol dependent and correlates with individual well-being. J. Neurosci. Res. 99, 2271–2286. https://doi.org/10.1002/jnr.24898.

Lomen-Hoerth, C., Anderson, T., Miller, B., 2002. The overlap of amyotrophic lateral sclerosis and frontotemporal dementia. Neurology 59, 1077–1079.

Kawashima, T., Doh-ura, K., Kikuchi, H., Iwaki, T., 2001. Cognitive dysfunction in patients with amyotrophic lateral sclerosis is associated with spherical or crescent-shaped ubiquitinated intraneuronal inclusions in the parahippocampal gyrus and

amygdala, but not in the neostriatum. Acta Neuropathol. 102, 467–472. https://doi.org/10.1007/s004010100398.
Kravitz, D.J., Saleem, K.S., Baker, C.I., Mishkin, M., 2011. A new neural framework for visuospatial processing. Nat. Rev. Neurosci. 12, 217–230. https://doi.org/10.1038/nrn3008.
Loewe, K., Machts, J., Kaufmann, J., Petri, S., Heinze, H.-J., Borgelt, C., Harris, J.A., Vielhaber, S., Schoenfeld, M.A., 2017. Widespread temporo-occipital lobe dysfunction in amyotrophic lateral sclerosis. Sci. Rep. 7, 40252. https://doi.org/10.1038/srep40252.
Lulé, D., Diekmann, V., Müller, H.-P., Kassubek, J., Ludolph, A.C., Birbaumer, N., 2010. Neuroimaging of multimodal sensory stimulation in amyotrophic lateral sclerosis. J. Neurol., Neurosurg. Psychiatry 81, 899–906. https://doi.org/10.1136/jnnp.2009.192260.
McGraw, K.O., Wong, S.P., 1996. Forming inferences about some intraclass correlation coefficients. Psychol. Methods 1, 30–46. https://doi.org/10.1037/1082-989X.1.1.30.
Menke, R.A.L., Proudfoot, M., Talbot, K., Turner, M.R., 2017. The two-year progression of structural and functional cerebral MRI in amyotrophic lateral sclerosis. NeuroImage Clin. 17, 953–961. https://doi.org/10.1016/j.nicl.2017.12.025.
Micheletti, S., Corbett, F., Atkinson, J., Braddick, O., Mattei, P., Galli, J., Calza, S., Fazzi, E., 2021. Dorsal and Ventral Stream Function in Children with Developmental Coordination Disorder. Frontiers in Human Neuroscience 15.
Mohammadi, B., Kollewe, K., Samii, A., Krampfl, K., Dengler, R., Münte, T.F., 2009. Changes of resting state brain networks in amyotrophic lateral sclerosis. Exp. Neurol. 217, 147–153.
Nasseroleslami, B., Dukic, S., Broderick, M., Mohr, K., Schuster, C., Gavin, B., McLaughlin, R., Heverin, M., Vajda, A., Iyer, P.M., Pender, N., Bede, P., Lalor, E.C., Hardiman, O., 2019. Characteristic increases in EEG connectivity correlate with changes of structural MRI in amyotrophic lateral sclerosis. Cereb Cortex 29, 27–41. https://doi.org/10.1093/cercor/bhx301.
Nolte, G., 2003. The magnetic lead field theorem in the quasi-static approximation and its use for magnetoencephalography forward calculation in realistic volume conductors. Phys. Med. Biol. 48, 3637.
Perez-Ortiz, C.X., Gordillo, J.L., Mendoza-Montoya, O., Antelis, J.M., Caraza, R., Martinez, H.R., 2021. Functional connectivity and frequency power alterations during P300 task as a result of amyotrophic lateral sclerosis. Sensors 21, 6801. https://doi.org/10.3390/s21206801.
Phukan, J., Pender, N.P., Hardiman, O., 2007. Cognitive impairment in amyotrophic lateral sclerosis. Lancet Neurol. 6, 994–1003.
Poujois, A., Schneider, F.C., Faillenot, I., Camdessanché, J., Vandenberghe, N., Thomas-Antérion, C., Antoine, J., 2013. Brain plasticity in the motor network is correlated with disease progression in amyotrophic lateral sclerosis. Hum. Brain Mapp. 34, 2391–2401.
Proudfoot, M., Bede, P., Turner, M.R., 2019. Imaging cerebral activity in amyotrophic lateral sclerosis. Front. Neurol. 9, 1148.
Proudfoot, M., Rohenkohl, G., Quinn, A., Colclough, G.L., Wuu, J., Talbot, K., Woolrich, M.W., Benatar, M., Nobre, A.C., Turner, M.R., 2017. Altered cortical beta-band oscillations reflect motor system degeneration in amyotrophic lateral sclerosis. Hum. Brain Mapp. 38, 237–254.
Rademakers, R., Neumann, M., Mackenzie, I.R., 2012. Advances in understanding the molecular basis of frontotemporal dementia. Nat. Rev. Neurol. 8, 423–434.
Rowland, L.P., 2001. How amyotrophic lateral sclerosis got its name: the clinical-pathologic genius of Jean-Martin Charcot. Arch. Neurol. 58, 512–515.
Sareen, E., Zahar, S., Van De Ville, D., Gupta, A., Griffa, A., Amico, E., 2021. Exploring MEG brain fingerprints: evaluation, pitfalls and interpretations. bioRxiv.
Shen, X., Finn, E.S., Scheinost, D., Rosenberg, M.D., Chun, M.M., Papademetris, X., Constable, R.T., 2017. Using connectome-based predictive modeling to predict individual behavior from brain connectivity. Nat. Protoc. 12, 506–518. https://doi.org/10.1038/nprot.2016.178.
Sorrentino, P., Rucco, R., Baselice, F., De Micco, R., Tessitore, A., Hillebrand, A., Mandolesi, L., Breakspear, M., Gollo, L.L., Sorrentino, G., 2021a. Flexible brain dynamics underpins complex behaviours as observed in Parkinson's disease. Sci. Rep. 11, 1–12.
Sorrentino, P., Rucco, R., Jacini, F., Trojsi, F., Lardone, A., Baselice, F., Femiano, C., Santangelo, G., Granata, C., Vettoliere, A., 2018. Brain functional networks become more connected as amyotrophic lateral sclerosis progresses: a source level magnetoencephalographic study. NeuroImage Clin. 20, 564–571.
Sorrentino, P., Rucco, R., Lardone, A., Liparoti, M., Troisi Lopez, E., Cavaliere, C., Soricelli, A., Jirsa, V., Sorrentino, G., Amico, E., 2021b. Clinical connectome fingerprints of cognitive decline. NeuroImage 238, 118253. https://doi.org/10.1016/j.neuroimage.2021.118253.
Sorriso, A., Sorrentino, P., Rucco, R., Mandolesi, L., Ferraioli, G., Franceschini, S., Ambrosanio, M., Baselice, F., 2019. An automated magnetoencephalographic data cleaning algorithm. Comput. Methods Biomech. Biomed. Eng. 22 (14), 1116–1125. https://doi.org/10.1080/10255842.2019.1634695.
Svaldi, D.O., Goñi, J., Abbas, K., Amico, E., Clark, D.G., Muralidharan, C., Dzemidzic, M., West, J.D., Risacher, S.L., Saykin, A.J., Apostolova, L.G., 2021. Optimizing differential identifiability improves connectome predictive modeling of cognitive deficits from functional connectivity in Alzheimer's disease. Hum. Brain Mapp. 42, 3500–3516. https://doi.org/10.1002/hbm.25448.
Trojsi, F., Monsurro, M.R., Esposito, F., Tedeschi, G., 2012. Widespread structural and functional connectivity changes in amyotrophic lateral sclerosis: insights from advanced neuroimaging research. Neural Plast. 2012.
Turner, M.R., Agosta, F., Bede, P., Govind, V., Lulé, D., Verstraete, E., 2012. Neuroimaging in amyotrophic lateral sclerosis. Biomark. Med. 6, 319–337.
Turner, M.R., Kiernan, M.C., 2012. Does interneuronal dysfunction contribute to neurodegeneration in amyotrophic lateral sclerosis? Amyotroph. Lateral Scler. 13, 245–250.
Van Veen, B.D., Van Drongelen, W., Yuchtman, M., Suzuki, A., 1997. Localization of brain electrical activity via linearly constrained minimum variance spatial filtering. IEEE Trans. Biomed. Eng. 44, 867–880.
Varoquaux, G., Raamana, P.R., Engemann, D.A., Hoyos-Idrobo, A., Schwartz, Y., Thirion, B., 2017. Assessing and tuning brain decoders: cross-validation, caveats, and guidelines. NeuroImage 145, 166–179.
Verstraete, E., Veldink, J.H., Mandl, R.C.W., van den Berg, L.H., van den Heuvel, M.P., 2011. Impaired structural motor connectome in amyotrophic lateral sclerosis. PLoS One 6, e24239.
Zhang, Y., Fang, T., Wang, Y., Guo, X., Alarefi, A., Wang, J., Jiang, T., Zhang, J., 2017. Occipital cortical gyrification reductions associate with decreased functional connectivity in amyotrophic lateral sclerosis. Brain Imaging Behav. 11, 1–7. https://doi.org/10.1007/s11682-015-9499-9.
Zhou, C., Hu, X., Hu, J., Liang, M., Yin, X., Chen, L., Zhang, J., Wang, J., 2016. Altered brain network in amyotrophic lateral sclerosis: a resting graph theory-based network study at voxel-wise level. Front. Neurosci. 10, 204. https://doi.org/10.3389/fnins.2016.00204.